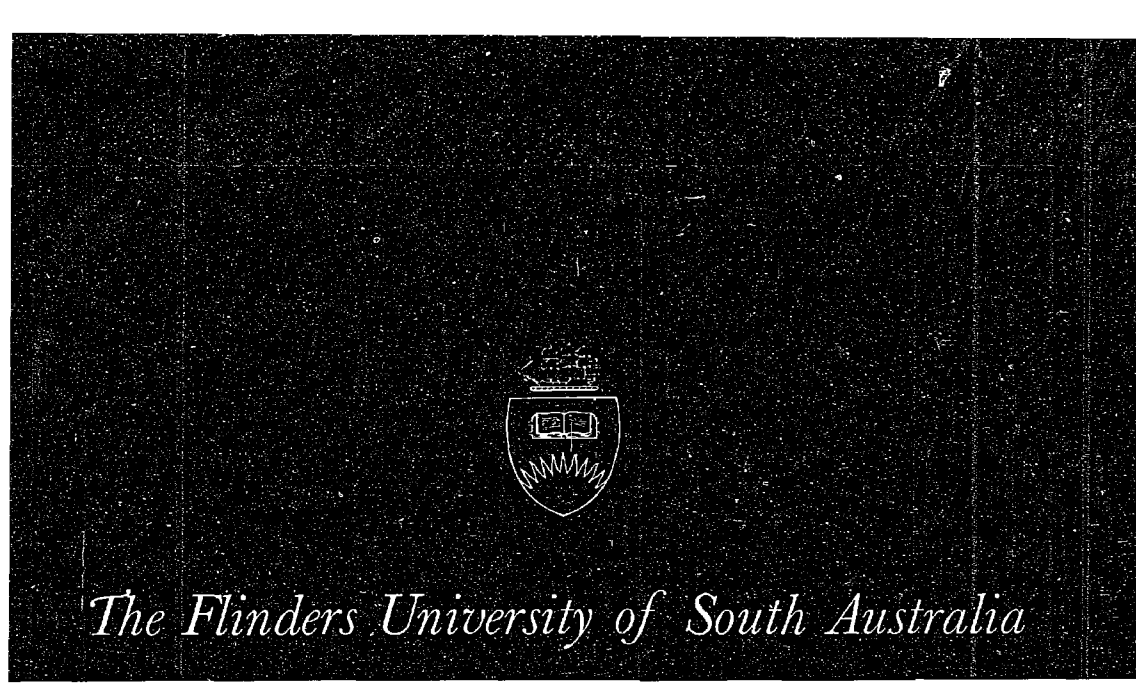

The Flinders University of South Australia

ELECTRONIC STRUCTURE OF MATERIALS CENTRE

(e,2e) Spectroscopy of Solids with Improved Energy Resolution

S. Canney, M.J. Brunger, I.E. McCarthy, P.J. Storer, S. Utteridge, M. Vos and E. Weigold

ESM-127 **March 1996**

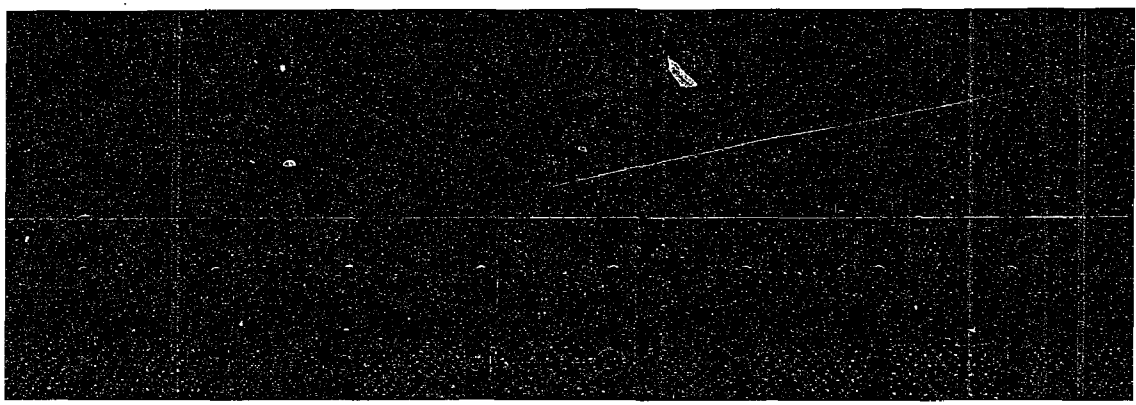

(e,2e) Spectroscopy of Solids With Improved Energy Resolution

S.A. Canney, M.J. Brunger, I.E. McCarthy, P.J. Storer *, S. Utteridge, M. Vos and E. Weigold †

Electronic Structure of Materials Centre, Flinders University of South Australia, GPO Box 2100, Adelaide S.A. 5001, Australia.

Abstract

A brief overview of the *(e,2e)* technique as applied to solids is reported, including the spectrometer used in these studies. In particular we describe how the energy resolution of our spectrometer has been improved by the addition of an electron monochromator for production of the incident electron beam. This monochromator is also discussed in some detail. Results obtained using the monochromated beam are compared with previous data collected with a standard electron-gun source.

I. INTRODUCTION

Many different spectroscopic techniques have provided detailed information on the electronic structure of materials. The type of information obtained depends on the measured parameters. Some very successful techniques that have been used in recent times are photoelectron spectroscopy [1], Compton scattering [2], positron annihilation [3] and *(e,2e)* electron momentum spectroscopy [4,5]. The performance of any of these techniques depends on

---

*Present Address: MCI Ltd., 40 Maple Ave., Forestville S. A. 5035, Australia.

†Present Address: Research School of Physical Sciences and Engineering, Australian National University, Canberra, Australia.

the precision with which the experimental results are obtained. In this paper we describe *how results from the (e,2e) technique benefit from the increased energy resolution obtained* by the addition of an electron monochromator to the coincidence spectrometer.

The *(e,2e)* technique allows the energy-momentum density of electrons in solids to be mapped directly. The very first *(e,2e)* experiment on solids by Amaldi *et al.* [6], had an energy resolution of 150 eV. In these experiments the different valence states of carbon could not be resolved, however they were able to resolve the core state from the valence states. It took a further decade before the energy resolution had improved by an order of magnitude. Indeed it was not until the experiments of Ritter *et al.* [7] , where the energy resolution had been increased to about 6 eV, that some structure of the valence bands could be resolved. More recently the spectrometer described by Storer *et al.* [8] obtained an energy resolution of $\approx$ 1.5 eV. This resolution has been improved further with the addition of an electron monochromator. In Fig. 1 we plot energy resolution as a function of time for *(e,2e)* experiments from solids in order to emphasize how the progression of technology has led to better energy resolution. All of the papers cited in Fig. 1 [6–13] have played a significant role in the development of *(e,2e)* spectroscopy of solids. At the same time the momentum resolution has improved considerably from the first experiments, down to 0.15 atomic units for our *(e,2e)* experiments. Moreover data collection efficiency has significantly increased over time, coincidence rates these days being improved by at least a factor of 100 over those of a decade ago. These developments thus make *(e,2e)* spectroscopy a very attractive technique for determining the electronic structure of materials.

The application of *(e,2e)* studies to solid targets has not been as rapid as those to gas-phase targets [4] due to the increased complexity of the interaction. The much higher density of the solid target requires more energetic electrons than gas phase experiments. However an advantage of having a higher target density is that less incident electron beam current is required to perform an *(e,2e)* experiment. For this reason it seemed quite feasible to monochromate the incident beam in our *(e,2e)* experiment. This has been done very successfully in the past for energy loss gas-phase experiments, see for example Trajmar

et al. [14], and an *(e,2e)* experiment on argon [15]. More recent experiments by Ibach [16] have been reported using an electron monochromator for energy loss experiments on solids. We note, however, that until this study there had not been an attempt to employ monochromated electrons in *(e,2e)* experiments on solids.

We report here on the *(e,2e)* spectroscopy of solids, the electron monochromator that we designed and built and some of the results that have been achieved thus far. These results clearly illustrate the improved performance of the spectrometer after the addition of the monochromator.

II. *(E,2E)* SPECTROSCOPY

The notation *(e,2e)* represents a process in which a high energy incident electron (energy E_o, momentum $\mathbf{k}_o$) knocks out a target electron, with subsequent detection of both outgoing electrons. These outgoing electrons are detected in coincidence to ensure they originated from the same scattering event. After detection of the *(e,2e)* event, the energies (E_f and E_s) and momenta ($\mathbf{k}_f$ and $\mathbf{k}_s$) of both outgoing electrons are determined. For convenience we have respectively labelled the outgoing electrons with the subscript *f* for the faster one and *s* for the slower one. The binding energy ε and momentum $\mathbf{q}$ of the target electron *before* the collision are given by the following conservation laws:

$$\varepsilon = E_o - E_s - E_f. \tag{1}$$

$$\mathbf{q} = \mathbf{p}_s + \mathbf{p}_f - \mathbf{p}_o. \tag{2}$$

Hence the *(e,2e)* technique is kinematically complete, that is all the kinematic information regarding the scattering event is obtained. During an *(e,2e)* experiment the energy-resolved electron momentum density is measured. In the independent particle approximation this is equal to the absolute square of the momentum space wavefunction ($|\phi(\varepsilon, \mathbf{q})|^2$), hence the common reference to 'wave-function mapping'. The *(e,2e)* technique therefore directly

determines the electron distribution in momentum space in the system of interest, and is consequently commonly referred to as electron momentum spectroscopy (EMS).

A. *(e,2e)* Spectroscopy of Solids

(e,2e) experiments on atoms and molecules are now well established. These measurements have been and continue to be performed successfully, for example see McCarthy and Weigold [17]. They are conducted with electron energies of the order of 1.5 keV. With respect to solid state targets the progression has been relatively slower due to complications that arise from the high density target samples. With solids one is also required to use a transmission mode in order to determine $|\phi(\varepsilon, q)|^2$ for all q, as is illustrated in Fig. 2 which shows the geometry used in the present measurements. This requirement means that the solid state targets must be very thin membranes ($\leq$ 200 Å) to enable the electrons to emerge from the back of the film. In spite of our targets being very thin they still have a higher density than a gaseous target (used in atomic and molecular studies) so that much higher electron energies are needed to avoid additional scattering. Indeed by making the samples as thin as practicable and maximising the electron beam energies we minimise the possibility of multiple scattering. A multiple scattering event occurs when any of the three electrons involved in the *(e,2e)* reaction undergoes either an elastic or inelastic scattering event other than the *(e,2e)* event. This is discussed in detail by Vos and Bottema [18]. Multiple scattering, as well as giving *(e,2e)* events with changed energies (due largely to inelastic events such as plasmon excitation) and momenta (due to both elastic and inelastic events) gives rise to increased background events and hence reduces the coincidence signal to random background ratio. This in term implies that longer collection times are required to obtain the desired high statistical accuracy on the data.

For solid-state targets there are infinitely many energy levels which constitute an energy band. Often rather subtle differences in the structure of various solids are the origin of different macroscopic properties. It is thus important to maximise the energy resolution in

order to obtain a detailed and accurate description of the energy bands. Hence the rationale for the continuing push for higher energy resolution in *(e,2e)* experiments on solids.

B. Solid-state *(e,2e)* spectrometer

The present *(e,2e)* spectrometer was designed for the study of solid targets with the aim of producing high coincidence count rates, good energy resolution and good momentum resolution. To achieve these criteria an *(e,2e)* coincidence spectrometer was built that utilises asymmetric, non-coplanar kinematics. A schematic representation detailing these points is shown in Fig. 2. For more details on this spectrometer see Storer *et al.* [8].

During a typical *(e,2e)* experiment on valence electrons the incident energy is 20 keV, with the energy of the fast electron nominally 18.8 keV and the energy of the slow electron about 1.2 keV. Constant polar angles of 14° and 76° degrees are used for the detection of the fast and slow electron respectively. With this geometry the measured momentum q for a coplanar event is zero. A range of azimuthal (out of the plane) angles are measured simultaneously. The fast electron is detected in a hemispherical analyser whilst a toroidal analyser detects the slow electron. Each electron analyser has a two-dimensional position-sensitive detector mounted at its exit, enabling a range of target electron binding energies ϵ and momenta q to be measured simultaneously. This is a major advantage as it greatly improves the *(e,2e)* coincidence rate.

The choice of asymmetric kinematics is very important for optimising the energy resolution. This follows as it makes it possible for the main high voltage power supply to be shared by both the electron gun and the fast electron analyser (see Fig. 3). This in turn ensures that any drift or ripple in this power supply is cancelled out, i.e. ϵ, as determined from Eqn. (1), is not affected by any drift or ripple and hence the energy resolution is not degraded. Only the stability of the other power supplies in Fig. 3 are of importance. Since these are only of the order of 1 keV, stabilities of 100 mV are easily obtained.

The choice of asymmetric kinematics also provides for smaller momentum transfer (K)

and hence a larger coincidence cross section since the electron-electron cross section is proportional to K^{-4} where :

$$K = p_o - p_f. \tag{3}$$

An additional advantage of using asymmetric kinematics is that the *(e,2e)* measurement is sensitive to the surface of the target facing the slow electron analyser. This arises because the escape depth of the slow electron is only about 20 Å, hence the *(e,2e)* event must occur in the outermost layers. The surface sensitive nature of the experiment makes it possible to perform adsorbate studies (Vos *et al.* [19]). It also makes possible the measurement of samples which have been evaporated onto a thin substrate by positioning the sample with the evaporated layer facing the slow electron analyser.

Previous *(e,2e)* measurements conducted with this spectrometer used an incident beam that was not monochromated [20–25]. The measurements revealed the energy-momentum densities of the valence bands of the material being studied. They also showed that provided samples can be produced with thickness' $\leq$ 200Å, the criterion of high coincidence count rates can be met. Typical *(e,2e)* measurements with this spectrometer take a few days to complete. The energy and momentum resolution have been measured in separate experiments and found to be 1.5 eV and $\leq$ 0.15 atomic units respectively (Storer *et al.* [8]). In order to improve the energy resolution and obtain sharper and more detailed EMS information for the targets of interest, the original electron gun was replaced by an electron monochromator.

III. ELECTRON MONOCHROMATOR

An electron monochromator was designed and constructed to produce an incident electron beam of appropriate flux but with better energy resolution than had previously been achieved in *(e,2e)* experiments on solids.

The incident beam used in the previously mentioned *(e,2e)* experiments was believed to be the major component restricting our energy resolution. This was verified by examining the

guns performance during elastic scattering experiments. In these experiments the incident beam energy is tuned to the energy of either of the two analysers i.e. these experiments are single electron scattering experiments. Typical results for these experiments are shown in Fig. 4. The full width at half-maximum (FWHM) of the elastic peak arising from the combination of the beam and hemispherical analyser and from the beam and toroidal analyser, was found to be about 0.7 eV in both cases. The FWHM of the elastic peak is given by

$$\Delta E_{(elastic)} = \sqrt{\Delta E^2_{(beam)} + \Delta E^2_{(analyser)}} \tag{4}$$

An important point to note here is that these elastic scattering experiments are performed with much lower beam currents (factor of 1000) than those used in an *(e,2e)* experiment. Under these circumstances, i.e. for experiments performed with low beam currents, we have $\Delta E_{beam} \approx \Delta E_{thermal}$ where $\Delta E_{thermal} \approx 2.54 k_B T$ = T/4570K eV. From source brightness considerations we estimate the temperature of the tungsten filament to be 2800 K, leading to a $\Delta E_{thermal} \approx 0.6$ eV (see Ibach [16] or Klemperer [26] for more details). This implies from (4) an energy resolution of about 0.4 eV for each analyser. When going from an elastic scattering experiment to an *(e,2e)* experiment the beam current must be increased, resulting in an even poorer energy resolution due to space charge effects. This is not the case when the beam is monochromated. The total coincidence energy resolution of the spectrometer during an *(e,2e)* measurement is determined by the addition of each component in quadrature, i.e.

$$\Delta E_{(e,2e)} = \sqrt{\Delta E^2_{(beam)} + \Delta E^2_{(FA)} + \Delta E^2_{(SA)}} \tag{5}$$

where *FA* and *SA* are the fast and slow electron analysers respectively. The measured *(e,2e)* energy resolution, without monochromation, of around 1.5 eV [8] and given $\Delta E_{(FA)} \approx \Delta E_{(SA)} \approx 0.4$ eV indicates from (5) that the incident beam is the major factor preventing improved energy resolution.

The electron monochromator is required to provide maximum energy resolution whilst maintaining sufficient beam current to perform *(e,2e)* experiments. The monochromator

consists of three major components, a gun lens stack, an energy selector (180° electrostatic deflector) and a target lens stack. A schematic view of the electron monochromator and the collision chamber which contains both analysers is shown in Fig. 5.

The design and method of construction of the present monochromator, including the relevant voltage supply modules for the individual electron-optic lens and hemispherical elements, was based on that developed for EMS studies on larger molecules [27]. Whilst both these monochromators employed hemispherical energy selectors and a cylindrical lens-element geometry, there are significant differences between them. These differences arose due to the particular, stringent, requirements of the present application of monochromated electrons to *(e,2e)* studies on solids. These include a beam spot size of diameter about 200 μm, zero beam angle at the target and superior momentum resolution. A full discussion of these points and the major design criteria of the present apparatus are given below.

A. Gun Lens Stack

The design of the gun lens stack (and for that matter the target lens stack) was based on our requirements that the beam at the the target had a small spot size, zero beam angle and high momentum resolution. These criteria were in general met by ensuring that in the design of the monochromator the magnification of the respective lenses was kept close to unity, the pencil angle divergences were minimised and the electron filling factor η of the lenses was always kept below 0.4. This latter criterion in turn minimised potential problems due to spherical aberration effects. The lenses were designed with the aid of Harting and Read [28]. A schematic of the gun lens stack is shown in Fig. 6.

The electron source is a tungsten hairpin filament mounted in a standard triode configuration. The triode configuration contains a Pierce element (G1) [29], an anode aperture (GA) and a collimating aperture (GA1) which also defines the entrance window to the first three cylinder lens GL1. Electrons that are thermionically emitted from the tungsten filament (cathode) are repelled from the source by applying a negative voltage to G1 (typically

-2.5 V). A positive potential of about 80 volts is applied to GA so that the electrons extracted from the cathode are focussed by GA onto GA1. All potentials listed are relative to the cathode potential unless otherwise stated. In addition a potential of 180 volts on GA1 is typically required to extract sufficient electrons from the source. We note that the major role of GA1 is to provide some initial collimation of the electron beam. The three cylinder lens GL1 (G/D = 0.1, A/D = 1.0, where G and A are the lens gaps [28] and D is the lens diameter, D = 10 mm) takes the electrons from GA1 and images them onto the physical defining aperture GA3 (ϕ = 0.6 mm) i.e. GA3 is placed at the image distance (Q) of GL1. All three element cylindrical lenses described in this paper have the same values of G,A and D. The next three cylinder lens GL2 decelerates and focusses the electron beam from GA2 (ϕ = 0.8 mm) and images it onto a virtual aperture at the entrance plane of the energy selector. By placing GA2 at the object distance (P) of GL2 we have ensured that an exchange of window and pupil takes place. In addition we have separated the two "field-free" apertures GA2 and GA3 by as much as practicable to minimise η, aberration effects and the pencil angles of the beam at the selector entrance. Note that by adopting the "window-pupil" exchange configuration we also effectively ensure a zero beam angle at the selector entrance.

Theoretical operating potentials of the three elements in GL1 are V1 = 180 Volts; V2 = 480 Volts; V3 = 60 Volts. For the second lens system GL2 the corresponding potentials are V1 = 60 Volts; V2 = 150 Volts; V3 = 30 Volts. The two deflector sets in the gun lens stack are used purely to steer the electron beam through the stack, they do not have any focussing action on the electron beam.

B. Energy Selector

The energy selector is the core of any electron monochromator. An electrostatic hemispherical analyser was chosen as the energy selector for our monochromator. The report of Brunt *et al.* [30] described a 180° electrostatic deflector which had the feature of the elec-

trostatic deflectors being slitless, that is, the entrance and exit planes of the selector did not contain any physical apertures. This feature is also utilised in the energy selector reported here. The main advantage of virtual apertures over physical apertures is that the beam does not have to pass through an extra set of apertures with the associated current loss. Furthermore there are no additional disturbances to the electrostatic field at the entrance and exit of the selector. A full discussion of these fringe field effects can be found in Brunt *et al.* [30]. The energy selector focusses the electron beam from the entrance to the exit plane with a magnification of one.

The selector is constructed out of two aluminium hemispheres, the radius of the inner hemisphere, r_{inner} = 38 mm and the radius of the outer hemisphere, r_{outer} = 62 mm. This gives a mean radius of the hemispherical deflector of r_o = 50 mm. The major constraint on the size of the hemispheres is the physical size of the vacuum chamber. From Imhof *et al.* [31] the potentials that need to be applied to the inner and outer hemispheres are 49.0 Volts and 18.4 Volts respectively, for a mean analysing potential of V_o = 30 volts. It is desirable to be able to vary V_o in order to optimize the energy resolution and beam intensity. The full energy width at half maximum, ΔE_{beam}, is given by Read *et al.* [32] as

$$\Delta E_{beam} = V_o\left(\alpha_{1/2}\frac{r_s}{L_s} + \beta_{1/2}\theta_s^n\right) \tag{6}$$

where r_s = radius of the beam at both the entrance and exit of the selector, n=2 for a hemispherical selector [32], L_s = representative dimension of the selector which is consistently taken to be the distance in a straight line between the entrance and exit positions($\equiv 2r_o$) and θ_s = pencil angle at the selector entrance. From Read *et al.* [32], the functions $\alpha_{1/2}$ and $\beta_{1/2}$ are dependent on θ_s, r_s and L_s. Using this information they are found to be 1.63 and 0.23 for a 180° deflector. For our case, with V_o = 30 eV, r_s = 0.877 mm, L_s = 100 mm and θ_s = 6.26 mrads, we get from (8) a theoretically determined energy resolution $\Delta E_{(beam)}$ = 0.43 eV. This compares favourably to that obtained by Storer *et al.* [8], without monochromation, of $\Delta E_{(beam)}$ = 1.39 eV. Note the value 0.43 eV should be considered as a lower bound to that which is attainable experimentally due to the existance of space charge and fringe field

effects that are not accounted for in equation (8).

C. Target Lens Stack

The target lens stack is required to accelerate the beam from 30 eV kinetic energy up to 20 keV to meet the requirements for the incident beam used in an *(e,2e)* experiment. This acceleration is performed in three stages. The electron beam is first accelerated from 30 eV to 300 eV via a three element cylinder lens TL1. Another three element cylinder lens, TL2, accelerates the beam from 300 eV to 2 keV. The final acceleration from 2 keV to 20 keV is undertaken by a two element cylinder lens. This lens is labelled acceleration stage in Fig. 5. A schematic of the target lens stack is also shown in Fig. 6.

The target lens stack, consisting of lenses TL1 and TL2, transports the beam from the selector exit to the object position of the acceleration stage, before final acceleration. In our design of this lens stack we have also incorporated two defining apertures (TA1 and TA2) in the field free region and we have again configured them for window-pupil exchange. To achieve this exchange of window and pupil we require the electron beam to be focussed from the selector exit plane to the second defining aperture TA2 (ϕ = 0.3 mm) placed at the image distance of TL1, whilst the first defining aperture TA1 (ϕ = 0.3 mm) is at the object distance of TL2. Further we ensured that TA2 remains close to the first focal plane of TL2 to produce a zero beam angle for later imaging and acceleration by the acceleration stage. In addition the aperture diameters of TA1 and TA2 were deliberately chosen to be very small to minimise the beam pencil angles. Typical operating potentials for the lens stack TL1 are V1 = 30 Volts; V2 = 90 Volts; V3 = 300 Volts, while the corresponding potentials for TL2 are V1 = 300 Volts; V2 = 240 Volts; V3 = 2000 Volts.

In practice small deviations from all the voltages listed are sometimes required to produce an electron beam with sufficient current for an *(e,2e)* experiment. As in the gun lens stack, two sets of deflectors are placed in the target lens stack to guide the electron beam through the stack. The final acceleration from 2 keV to 20 keV is performed by the two cylinder lens

labelled acceleration stage (D1 = 50 mm , D2 = 25 mm). The specification of zero beam angle is also achieved by this two cylinder lens (beam rays are parallel to each other). The resultant electron beam leaves the monochromator (exit of acceleration stage) with a kinetic energy of 20 keV.

From the exit of the monochromator the beam is still required to travel a further 500 mm before striking the target. To effectively transport the beam over this distance an einzel lens is placed just inside the main chamber (about 200 mm after acceleration stage). An einzel lens consists of three cylindrical elements which are operated with elements V1 and V3 at the same potential. For our application the outer two elements are at ground potential and the inner lens element is at positive 12 kV (relative to ground). The electron beam exiting the einzel lens then passes through a collimating tube which contains two apertures. These collimating apertures are used to further minimize the divergence of the electron beam and hence improve the momentum resolution. The final result is a 20 keV electron beam with a spot size of around 200 μm in diameter and a divergence of 2 mrads (corresponding to a momentum spread of 0.08 a.u.). This electron beam is then used to instigate the *(e,2e)* reaction.

IV. EXPERIMENTAL RESULTS

With the above arrangement the beam is stable in time and beam currents of around 100 nano-amps in the Faraday cup are achieved. This is more than adequate for *(e,2e)* experiments, which typically use about 60 nano-amps depending on target thickness. Elastic scattering experiments have been conducted, as with the previous electron gun, and these show an improvement in the FWHM of the elastic peak of 0.2 eV for each analyser. The true test of the monochromator's performance, however, is an experimental measurement of the total energy resolution under *(e,2e)* conditions.

An experiment on the 1s core state of carbon from an amorphous target using the previous electron gun (not monochromated) was reported by Caprari *et al.* [33]. The raw data showed

a narrow 1s core peak with a FWHM of 1.9 eV. This experiment has been repeated with a monochromated incident beam and the FWHM of the carbon 1s peak was determined to be 1.2 eV. A significant improvement has been observed here, although an estimate of the total resolution (including linewidths) could not be achieved as this peak is already better resolved than the linewidth measured by Lascovich *et al.* [34] from amorphous carbon using photoemission. Sette *et al.* [35] report that the line width of the 1s peak is much less for crystalline graphite targets. In this case the line width contribution should only be of the order of 0.2 eV. For this reason a core state measurement was conducted on a natural graphite sample (estimated thickness of 100 Å). We used the same sample preparation method as described by Vos *et al.* [20] for highly oriented pyrolytic graphite (HOPG) samples. The raw data from this *(e,2e)* experiment shows a narrow 1s peak with a FWHM of 0.9 eV. The raw data for each of these three experiments are shown in Fig. 7. Considering the contribution to the linewidth of the peak in Fig. 7(c) to be minimal, we have a long term experimental resolution for the whole system (electron gun, both analysers and power supplies) of 0.90 eV. The inclusion of the electron monochromator has thus clearly improved the resolution quite significantly.

The benefits of the electron monochromator become even more obvious in the *(e,2e)* experiments on fullerenes (C_{60}). A fullerene sample was prepared by evaporating 40 Å of C_{60} (obtained from MER Corporation, Arizona as a powder) onto a thin (60 Å) amorphous carbon sample. An *(e,2e)* experiment was also performed on a fullerene sample prepared in an identical fashion, before the monochromator was placed on-line. The significant improvement in the energy resolution is clearly illustrated in this experiment. The comparison of these two *(e,2e)* experiments is shown in Fig. 8. The improved energy resolution with the electron monochromator makes it possible to resolve significant structure in the valence band which was not observed with the previous electron gun.

The improved energy resolution has obviously enhanced some structural features in the C_{60} energy plots. The objective of *(e,2e)* spectroscopy is to directly measure the energy-resolved momentum densities. In Fig. 9 we show the momentum densities which correspond

to the outermost valence band states of C_{60}. There is a clear shift in the peak positions towards zero momentum with increasing binding energy. Energy shifts in large molecules appear to resemble the dispersion that is observed in solids. This is discussed in detail by Vos and McCarthy [36]. Thus the increased energy resolution makes it also possible to measure the development of the momentum distributions as a function of binding energy. A detailed discussion of the C_{60} measurements will be given by Utteridge *et al.* [37].

V. CONCLUSION

This paper presents a discussion on *(e,2e)* spectroscopy as applied to solid-phase targets. A description is given of the asymmetric non-coplanar spectrometer. In particular we have outlined how the energy resolution of the system can be significantly improved by the incorporation of an electron monochromator. Preliminary *(e,2e)* experiments with the monochromator on the carbon 1s core state and on fullerenes are reported. These experiments show an improvement in the energy resolution by almost a factor of two, the present long term energy resolution being 0.90 eV.

ACKNOWLEDGMENTS

The authors would like to thank the staff of the Electronic Structure of Materials Centre for their invaluable contributions to these *(e,2e)* experiments. Thanks also to Dr. Peter Teubner for meaningful discussions. The Electronic Structure of Materials Centre is supported by a grant of the Australian Research Council.

REFERENCES

[1] F.J. Himpsel. *Advan. Phys.*, 32:1, 1983.

[2] M.J. Cooper. *Rep. Prog. Phys.*, 48:415, 1985.

[3] S. Berko, Proc. Int. School of Physics-Enrico Fermi, Varenna 1981, W. Brandt, and A. Dupasquier. Eds. North Holland Pub. Co., 1983.

[4] I.E. McCarthy and E. Weigold. *Rep. Prog. Phys.*, 54:789, 1991.

[5] I.E. McCarthy and E. Weigold. *Electron-atom collisions.* C.U.P., Cambridge, 1995.

[6] U. Amaldi Jr., A. Egidi, R. Marconero, and G. Pizzella. *Rev. Sci. Instrum.*, 40:1001, 1969.

[7] A.L. Ritter, J.R. Dennison, and R. Jones. *Phys. Rev. Lett.*, 53:2054, 1984.

[8] P. Storer, R.S. Caprari, S.A.C. Clark, M. Vos, and E. Weigold. *Rev. Sci. Instrum.*, 65:2214, 1994.

[9] R. Camilloni, A. Guardini-Guidoni, R. Tiribelli, and G. Stefani. *Phys. Rev. Lett.*, 29:618, 1972.

[10] N.M. Persiantseva, N.A. Krasil'nikova, and V.G Neudachin. *Sov. Phys. JETP*, 49:530, 1979.

[11] C. Gao, A.L. Ritter, J.R. Dennison, and N.A.W. Holzwarth. *Phys. Rev. B*, 37:3914, 1988.

[12] P. Hayes, J.F. Williams, and J. Flexman. *Phys. Rev. B*, 43:1928, 1991.

[13] J. Lower, S.M. Bharathi, Y. Chen, K.J. Nygaard, and E. Weigold. *Surf. Sci.*, 251/252:213, 1991.

[14] S. Trajman, D.F. Register, and A. Chutjian. *Phys. Rep.*, 97:219, 1983.

[15] J.F. Williams and B.A. Willis. *J. Phys. B*, 7:L51, 1974.

[16] H. Ibach. *Electron Energy Loss Spectrometers.* Springer-Verlag, Berlin, 1991.

[17] I.E. McCarthy and E. Weigold. *Rep. Prog. Phys.*, 51:299, 1988.

[18] M. Vos and M. Bottema. *Phys. Rev. B*, to be published.

[19] M. Vos, S.A. Canney, P. Storer, I.E. McCarthy, and E. Weigold. *Surf. Sci.*, 327:387, 1995.

[20] M. Vos, P. Storer, S.A. Canney, A.S. Kheifets, I.E. McCarthy, and E. Weigold. *Phys. Rev. B*, 50:5635, 1994.

[21] M. Vos, P.J. Storer, Y.Q. Cai, I.E. McCarthy, and E. Weigold. *Phys. Rev. B*, 51:1866, 1995.

[22] Y.Q. Cai, M. Vos, P. Storer, A.S. Kheifets, I.E. McCarthy, and E. Weigold. *Phys. Rev. B*, 51:3449, 1995.

[23] M. Vos, P.J. Storer, Y.Q. Cai, A.S. Kheifets, I.E. McCarthy, and E. Weigold. *J. Phys. Condensed Matter*, 7:279, 1995.

[24] Y.Q. Cai, M. Vos, P. Storer, A.S. Kheifets, I.E. McCarthy, and E. Weigold. *Solid State Comm.*, 95:713, 1995.

[25] P. Storer, Y.Q. Cai, S.A. Canney, S.A.C. Clark, A.S. Kheifets, I.E. McCarthy, S. Utteridge, M. Vos, and E. Weigold. *J. Phys. D: Appl. Phys.*, 28:2340, 1995.

[26] O. Klemperer. *Electron Optics 3rd ed.* Cambridge University Press, 1971.

[27] G.B Hewitt, G. Cotrell, and M.J. Brunger. *Meas. Sci. Tech.*, to be published.

[28] E. Harting and F.H. Read. *Electrostatic Lenses.* Elsevier, Amsterdam, 1976.

[29] J.R. Pierce. *Theory and Design of Electron Beams.* Van Nostrand, Toronto, 1949.

[30] J.N.H. Brunt, F.H. Read, and G.C. King. *J. Phys. E: Sci. Instrum.*, 10:134, 1977.

[31] R.E. Imhof, A.Adams, and G.C. King. *J. Phys. E: Sci. Instrum.*, 9:138, 1976.

[32] F.H. Read, J. Comer, R.E. Imhof, J.N.H. Brunt, and E. Harting. *J. Elect. Spect. and Rel. Phen.*, 4:293, 1974.

[33] R.S. Caprari, S.A.C. Clark, I.E. McCarthy, P. Storer, M. Vos, and E. Weigold. *Phys. Rev. B*, 50:12078, 1994.

[34] J.C. Lascovich, R. Giorgi, and S. Scaglione. *Appl. Surf. Sci.*, 47:17, 1991.

[35] F. Sette, G.K. Wertheim, Y. Ma, G. Meigs, S. Modesti, and C.T. Chen. *Phys. Rev. B*, 41:9766, 1990.

[36] M. Vos and I.E. McCarthy. *Rev. Mod. Phys.*, 67:713, 1995.

[37] S.Utteridge, M. Vos, S.A. Canney, P.J. Storer, A.S. Kheifets, I.E. McCarthy, and E. Weigold to be published.

FIGURES

FIG. 1. Plot of the the log of the energy resolution (eV) against time (years), for *(e,2e)* measurements on solids. The numbers are those as cited in the list of references.

FIG. 2. *Schematic representation of the geometry of the (e,2e) experiments [7]. In (a) we show* the range of angles measured. In (b) the sample orientation with respect to all three electron beams is shown. Most structural information is obtained from the shaded area of the sample since the slow electron has the smallest mean free path.

FIG. 3. The configuration of the high voltage power supplies used to define the beam energies for asymmetric kinematics [7]. The sharing of the main high voltage supply allows energy drifts to be cancelled out.

FIG. 4. *Electron energy loss spectra from a 100 Å amorphous carbon target taken without the* electron monochromator. In (a) nominally 18.8 keV incident energy in which the fast electrons are detected at $\theta_f = 14°$. In (b) nominally 1.2 keV incident energy in which the slow electrons are detected at $\theta_s = 76°$. Energy loss spectra collected after the inclusion of the electron monochromator showed an improvement of 0.2 eV FWHM for each electron analyser.

FIG. 5. Overall view of the electron monochromator mounted in its vacuum chamber. The main acceleration stage is also shown. The main chamber which houses the fast and slow electron *analysers is shown attached to the monochromator*

FIG. 6. Schematic of each of the lens stacks in the monochromator, in (a) the gun lens stack is shown and in (b) the target lens stack is shown. A basic ray trace of the electron beam in each lens stack, indicating focussing positions is also shown.

FIG. 7. Core state measurements of the 1s momentum integrated binding energy spectra for (a) an amorphous carbon sample with a non-monochromated incident beam, (b) an amorphous carbon sample with a monochromated incident beam and (c) from a natural graphite sample with monochromated incident beam

FIG. 8. Comparison of momentum integrated binding energy spectra of evaporated C_{60} with (a) an incident beam that is not monochromated and (b) a monochromated incident electron beam.

FIG. 9. Energy integrated momentum distributions of evaporated C_{60} for the outermost binding energy peaks. Arrows are shown to indicate the peak positions at each energy. The dispersion of these peaks is evident.

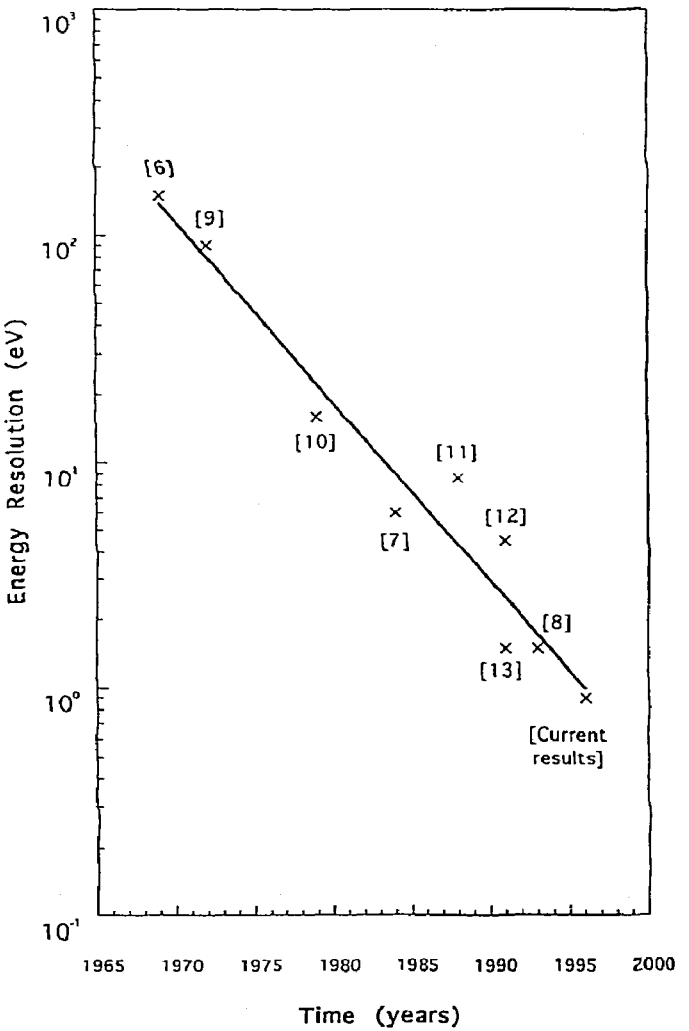
Energy Resolution (eV)
10³
10²
10¹
10⁰
10⁻¹
[6]
[9]
[10]
[11]
[12]
[7]
[8]
[13]
[Current results]
1965
1970
1975
1980
1985
1990
1995
2000
Time (years)

Fig 1

Fig 2

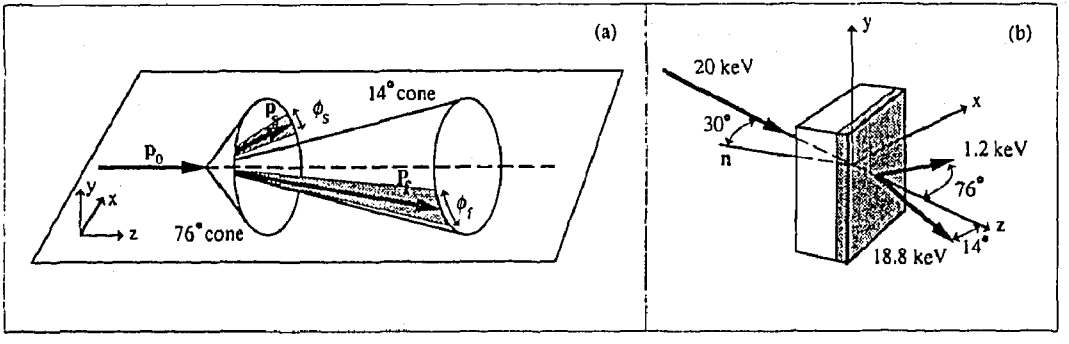
(a)
14° cone
p_s
ϕ_s
p_0
p_f
ϕ_f
y
x
z
76° cone
(b)
y
20 keV
30°
n
x
1.2 keV
76°
z
14°
18.8 keV

Fig 3

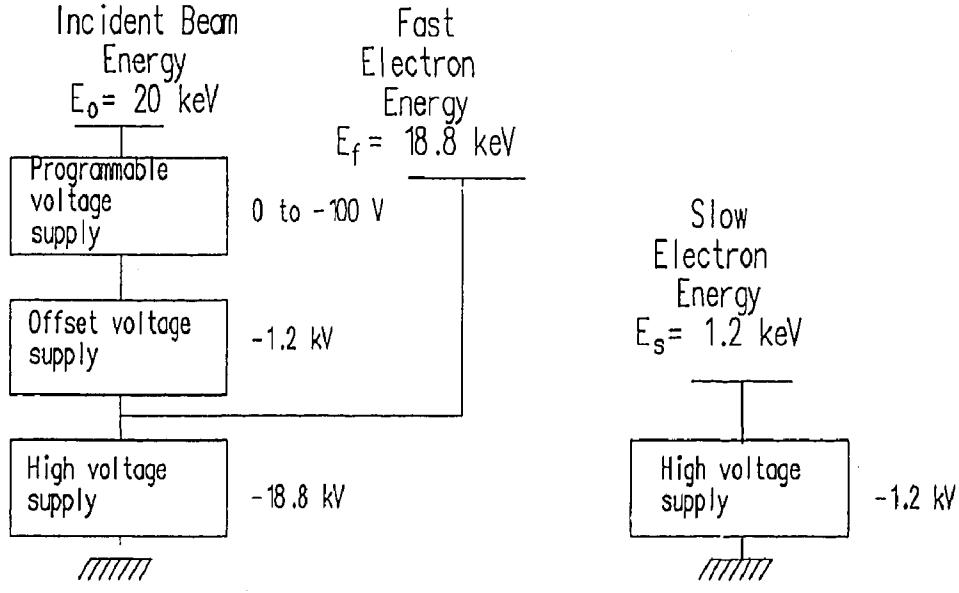
Incident Beam Energy
E_o = 20 keV
Fast Electron Energy
E_f = 18.8 keV
Programmable voltage supply
0 to -100 V
Offset voltage supply
-1.2 kV
High voltage supply
-18.8 kV
Slow Electron Energy
E_s = 1.2 keV
High voltage supply
-1.2 kV

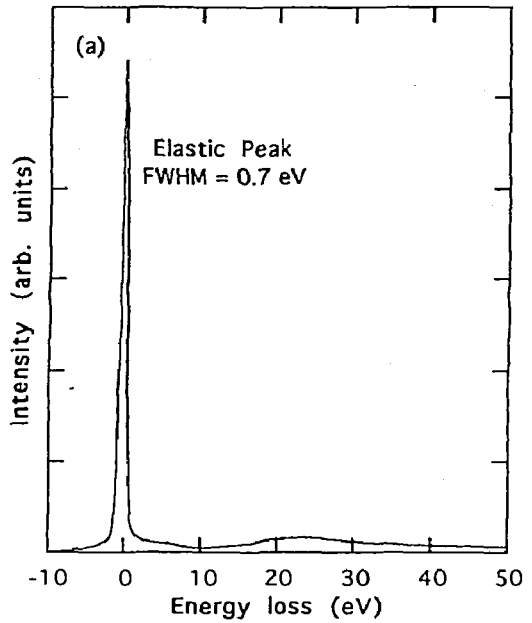
(a)
Elastic Peak
FWHM = 0.7 eV
Intensity (arb. units)
-10
0
10
20
30
40
50
Energy loss (eV)

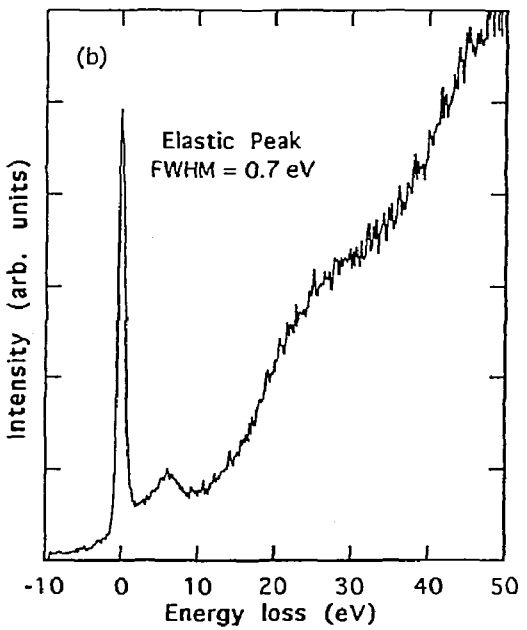
(b)
Elastic Peak
FWHM = 0.7 eV
Intensity (arb. units)
-10
0
10
20
30
40
50
Energy loss (eV)

Fig 4

Fig 5

Slow electron
detector
Electron
monochromator
Acceleration
stage
Einzel Lens
Collimator
Sample
Filament
Fast electron
detector

(a)

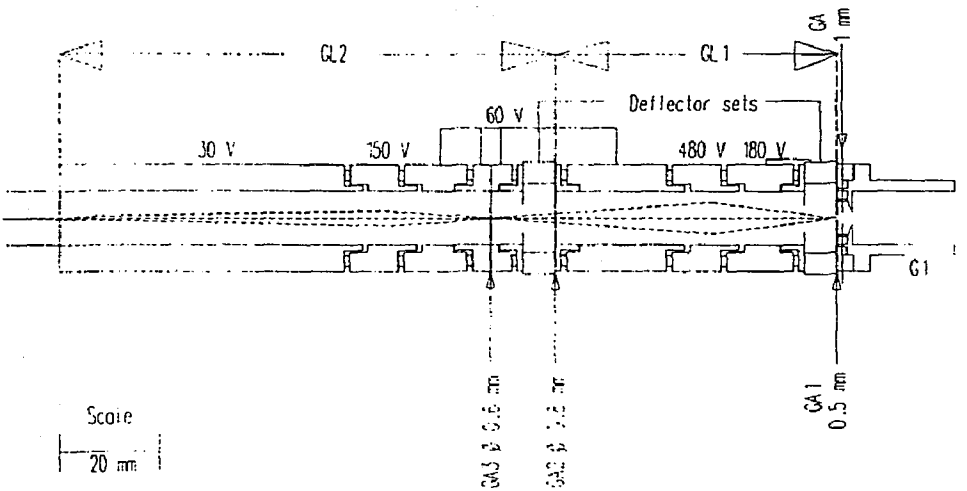
QL2
QL1
GA
1 mm
Deflector sets
60 V
30 V
150 V
480 V
180 V
G1
GA1
0.5 mm
Scale
20 mm

(b)

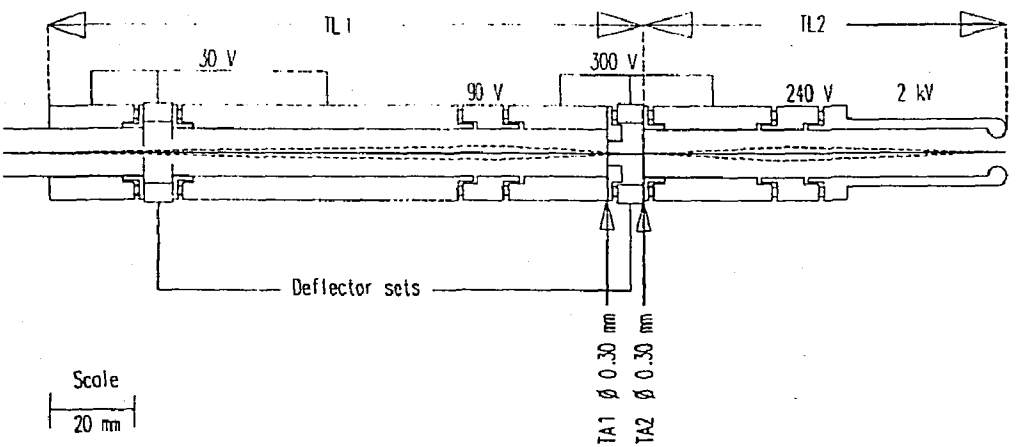
TL1
TL2
30 V
90 V
300 V
240 V
2 kV
Deflector sets
TA1 Ø 0.30 mm
TA2 Ø 0.30 mm
Scale
20 mm

Fig 6

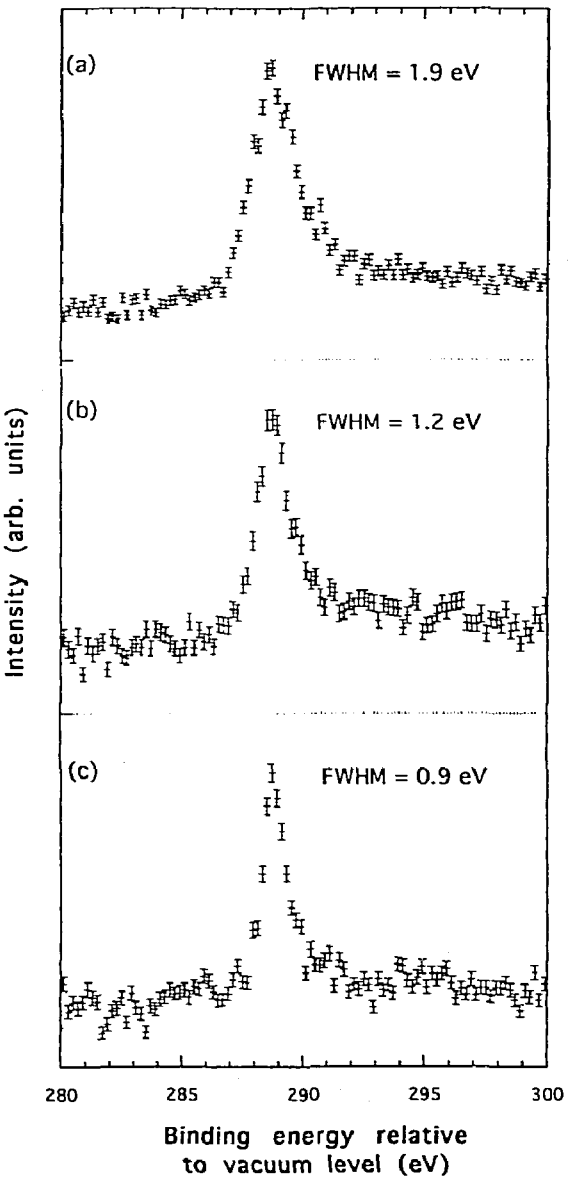
(a)
FWHM = 1.9 eV
(b)
FWHM = 1.2 eV
(c)
FWHM = 0.9 eV
Intensity (arb. units)
280
285
290
295
300
Binding energy relative
to vacuum level (eV)

Fig 7

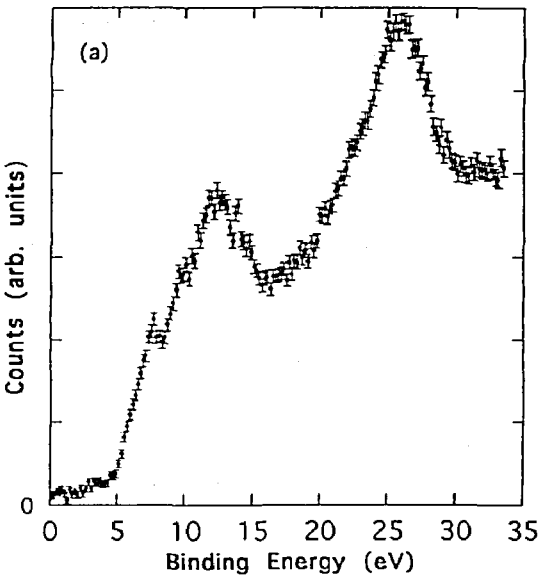
(a)
Counts (arb. units)
0
0 5 10 15 20 25 30 35
Binding Energy (eV)

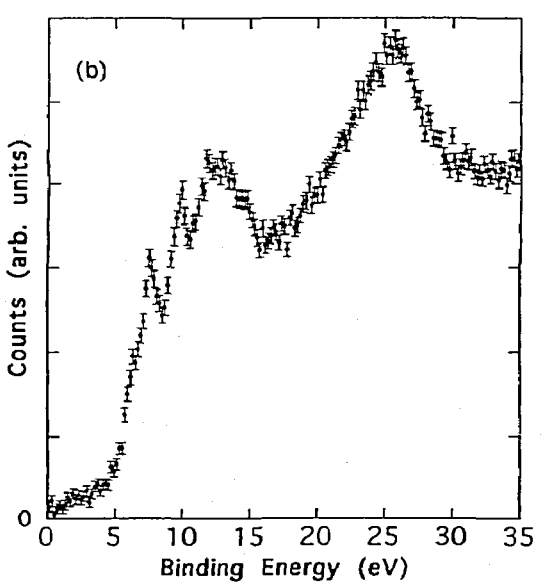
(b)
Counts (arb. units)
0
0 5 10 15 20 25 30 35
Binding Energy (eV)

Fig 8.

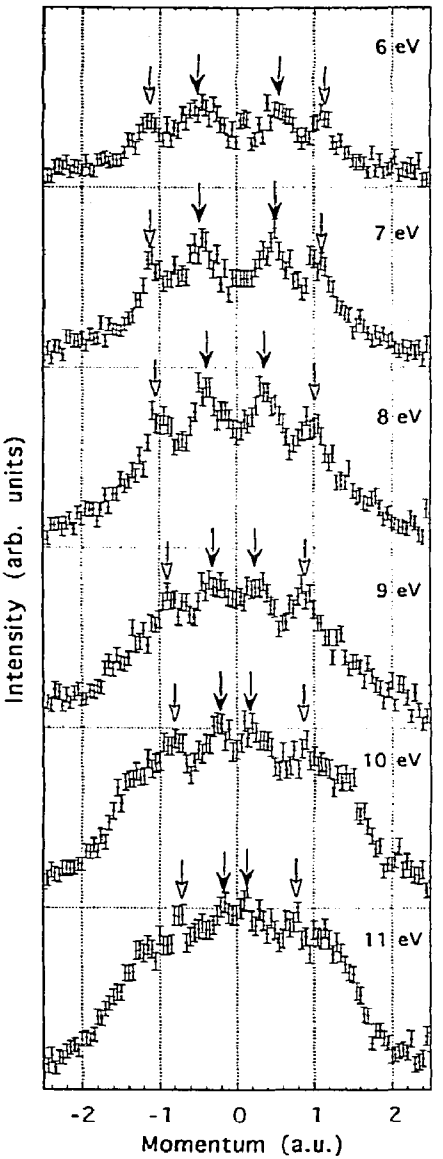
6 eV
7 eV
8 eV
9 eV
10 eV
11 eV
Intensity (arb. units)
-2
-1
0
1
2
Momentum (a.u.)

Fig 9.